Experimental Studies of Scale Effects on the Shear Behaviour of Rock Joints

S. BANDIS*
A. C. LUMSDEN*
N. R. BARTON†

The effect of scale on the shear behaviour of joints is studied by performing direct shear tests on different sized replicas cast from various natural joint surfaces. The results show significant scale effects on both the shear strength and deformation characteristics. Scale effects are more pronounced in the case of rough, undulating joint types, whereas they are virtually absent for planar joints. The key factor is the involvement of different asperity sizes in controlling the peak behaviour of different lengths of joints. It is shown that as a result both the joint roughness coefficient (JRC) and the joint compression strength (JCS) reduce with increasing scale. The behaviour of multiple jointed masses with different joint spacings is also considered. It is found that despite unchanged roughness, jointed masses consisting of many small blocks have higher peak shear strength than jointed masses with larger joint spacing. These scale effects are related to the changing stiffness of a rock mass as the block size or joint spacing increases or decreases. Economic methods for obtaining scale-free estimates of shear strength are described.

INTRODUCTION

The choice of an appropriate joint test-size during a shear strength investigation is generally based on both economic and technical considerations. The high cost of large scale conventional shear tests often leads to the relatively cheaper alternative of laboratory testing of small joint samples. However, small samples usually represent only a fraction of the natural joint exposures and such tests often yield unrepresentative data. Schneider [1] notes the reluctance of practicing engineers to apply friction values determined on 'laboratory'-size samples, a situation that often leads to more or less arbitrary reductions of friction angles (peak or residual) by 1 3 to 1 2 of their measured value.

The potential influence of joint test-size on measurements of shear strength has often been pointed out [2–5]. However, few systematic studies of the scale effect have been reported, and existing data from small and large scale tests are extremely limited and often inconclusive. One reason is that large in-situ shear tests are generally reserved for the most critical situations such as infilled joints, shear zones etc., where scale effects appear to be absent [3, 6, 7]. This is to be expected in those cases with a thickness of infilling larger than the roughness amplitude.

Comparisons of data from unfilled joints present a confusing picture because some tests indicate no scale effect [8], whereas in other cases the scale effect is either 'positive' [9] or 'negative' [10]. 'Negative' scale effects are often the result of dissimilar roughness on the small and large joints. For instance, in the case of Locher and Rieder's tests the laboratory samples were described as smooth, whereas the in-situ tested joints had undulating surfaces with amplitudes of ±2 cm. This could explain why the in-situ peak friction angle was 5° higher than that measured in the laboratory. Brown et al. [11] also found that the peak shear strength of artificially parted cleavage planes in slate increased as the sample areas increased from 60 to 1000 cm². Those authors noted that parting of the slate blocks produced surfaces 'stepping' from one cleavage plane to another. As would be expected, this effect became more marked as the sample size increased and produced 'rougher' surfaces with higher strength.

Different sizes of joint samples with similar roughness have shown 'positive' scale effects. A series of field shear tests by Pratt et al. [9] on a range of joint sizes in a weathered quartz diorite showed a 40% reduction in peak shear strength as the sample areas increased from 140 to 5000 cm². The family of shear stress (τ)–displacement (d_h) curves in Fig. 1 summarizes those experimental results. Barton & Choubey [12] measured tilt angles of 59° during self-weight sliding tests on a 45 cm long joint in granite. When the same sample was subdivided into eighteen blocks 10 cm in length, an average angle of 69° was obtained from a combination of tilt and push tests.

* Department of Earth Sciences, University of Leeds, Leeds LS2 9JT, England.
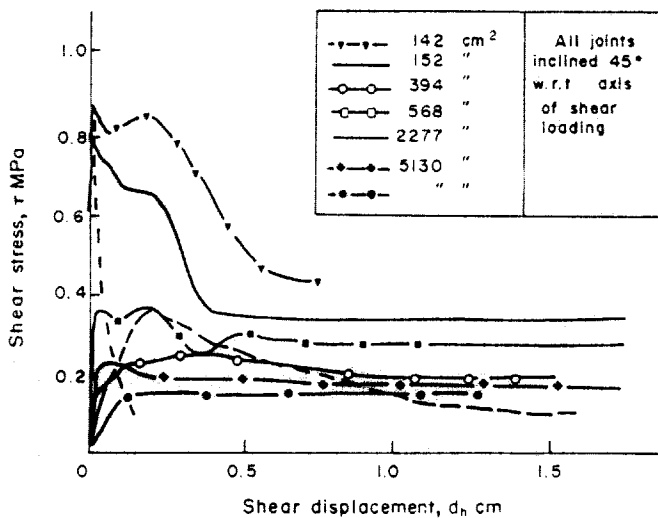† Terra Tek, 420 Wakara Way, Salt Lake City, UT 84108, U.S.A.; formerly Norwegian Geotechnical Institute, Oslo.

Fig. 1. Marked scale effects on the shear strength of joints in quarz diorite, after Pratt et al. [9].

Scale effects on shear strength have been explained in different ways. Pratt et al. [9] thought that the reduction in peak shear strength was due to decreasing actual contact area with increasing size of joint. They presumed that "... there would probably be no scale effect if the contact area of small and large joints was the same" and that such might be the case for unweathered, perfectly mating joints under high normal stress. Barton [13] interpreted the same results on the basis of a scale effect on the joint compression strength (JCS) operating on the different sized samples. In a subsequent publication Barton & Choubey [12] suggested that the joint roughness coefficient (JRC) presents another potential source of scale effect on shear strength. Back-analysis of their tilt tests showed that the JRC value of the 45 cm joint increased from 5.5 to 8.7 after the joint had been divided into smaller blocks.

This review shows that, to date, scale effects are only poorly understood. Any significant improvement in understanding would require answers to the following questions:

(i) Are scale effects on shear behaviour an intrinsic characteristic of rock joints*?

(ii) What is the mechanism of shearing at different scales, and what are the factors controlling the magnitude of any scale effect?

(iii) To what extent is individual joint behaviour relevant to the behaviour of rock masses?

EXPERIMENTAL PROCEDURE

The experimental procedure consisted of direct shear testing of various sized portions of replicas of joint surfaces. A rubber hot melt moulding compound of high resolution (Vinamold 9525/'Hard') was used to take precise impressions of the roughness from a variety of

natural joint surfaces in various rock types. Joint lengths used were between 36 to 40 cm., and moulds were prepared from both sides of the joint. A multicomponent brittle material was used to cast several model replicas of identical interlocking specimens from each pair of moulds. The degree of detailed reproduction of the natural joint roughness achieved in the cast model surfaces can be seen in Fig. 2.

Direct shear tests were carried out both on the full sized model and on other replicas after they had been subdivided into sets of smaller samples, each set representing a different average block size, 5–6, 10–12, or 18–20 cm in length. All sample sizes were tested in the same relative direction of shear and under precisely the same level of normal stress (σ_n).
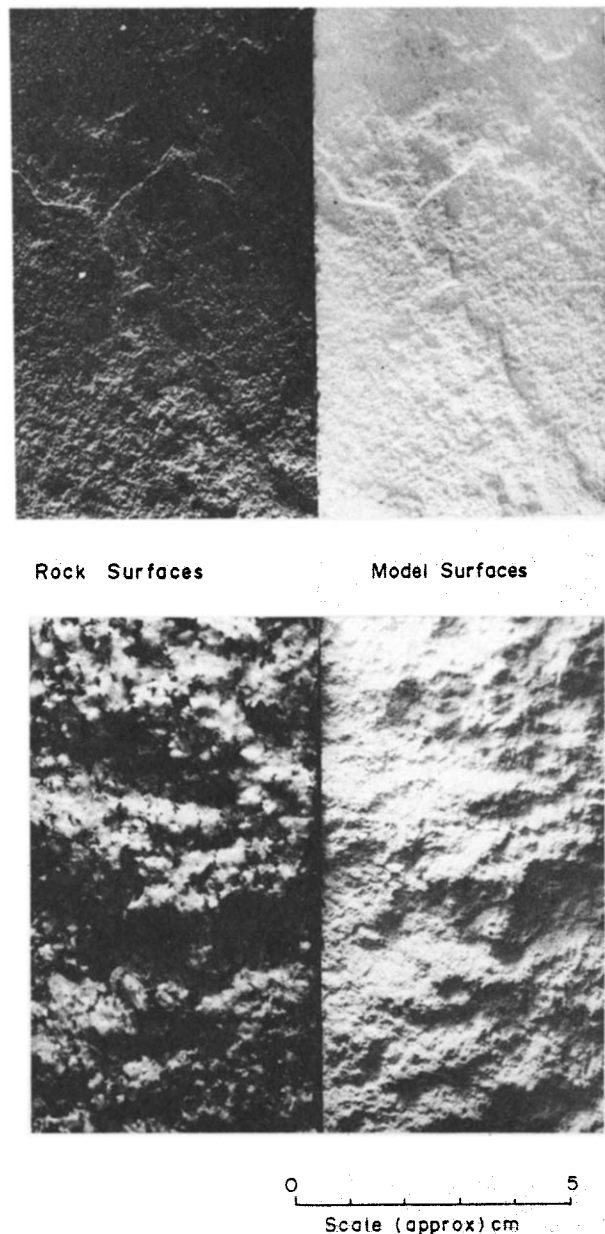

Rock Surfaces   Model Surfaces

Fig. 2. Photographs illustrating model joint surfaces (right side) obtained by casting the model material against rubber moulds of natural joint surfaces (left side).

---

* The term 'joint' will be used to describe all natural discontinuities in rock having zero tensile strength (100% persistence), an absence of soft infilling, and no previous history of displacement.

MECHANICAL PROPERTIES OF MODEL MATERIAL

The material used for casting the model joints consisted of a mixture of silver sand (d_{50} = 0.250 mm), calcined alumina (Burntisland grade, d_{50} = 0.062 mm), barytes, plaster of Paris and water combined in the following proportions by weight:

(barytes + alumina): sand = 1:2
alumina: barytes = 1:3
water: (barytes + alumina + sand) = 1:4

The joint replicas were oven-dried at 50°-55°C for 2-4 days depending on the sample size. Details of the development of the material are included elsewhere [14] and only a summary of the mechanical properties will be given here.

The uniaxial compression strength (σ_c) of the model material was measured on cylindrical specimens 25 mm dia and 50 mm in length. Strength was found to increase linearly with increasing plaster:filler (= barytes + alumina + sand) ratio, in the range from σ_c = 0.75 MPa (1:15) to σ_c = 3.45 MPa (1:7). The indirect tensile strength (σ_t) of the same mixtures was determined by the Brazilian method using solid discs 25 mm dia and 5 mm in thickness. Strength varied from 0.127 to 0.473 MPa. The axial stress (σ)-axial strain (ϵ) curves under uniaxial compression followed an essentially linear path up to approximately 3/4 of the failure stress, thence becoming slightly convex towards the stress axis. The axial strain (ϵ_f) at failure ranged from 0.33 to 0.4% and the tangent values of Young's Modulus at 50% of σ_c increased from 316 to 1305 MPa with increasing plaster:filler ratio in the above range.

The basic principles of model-prototype similitude (e.g. [15]) require that:

$$\Psi = \lambda \times \rho_p/\rho_m \qquad (1)$$

where

Ψ = stress scale factor
λ = geometric scale factor
ρ_p = density of prototype rock
ρ_m = density of model material

A geometric scale factor (λ) of 30 was adopted in this study and the density of the model material (ρ_m) was 1.85 g/cm³. Assuming a prototype rock density (ρ_p) of 2.5 g/cm³ the stress scale factor (Ψ) was defined as 40. The material finally used to cast the model joints simulated a prototype rock with uniaxial compression strength (σ_c) of 80 MPa, σ_c/σ_t = 6-7, $E/\sigma_c \sim$ 400 and ϵ_f = 0.35%. As an illustration of the strength and deformation properties of the model material compared to those of intact rock, the model values of σ_c and E were scaled up and plotted on the chart in Fig. 3 according to Deere and Miller's system of intact rock classification. As shown, the final model material fell in the zone of medium strength limestone and medium strength sandstone.
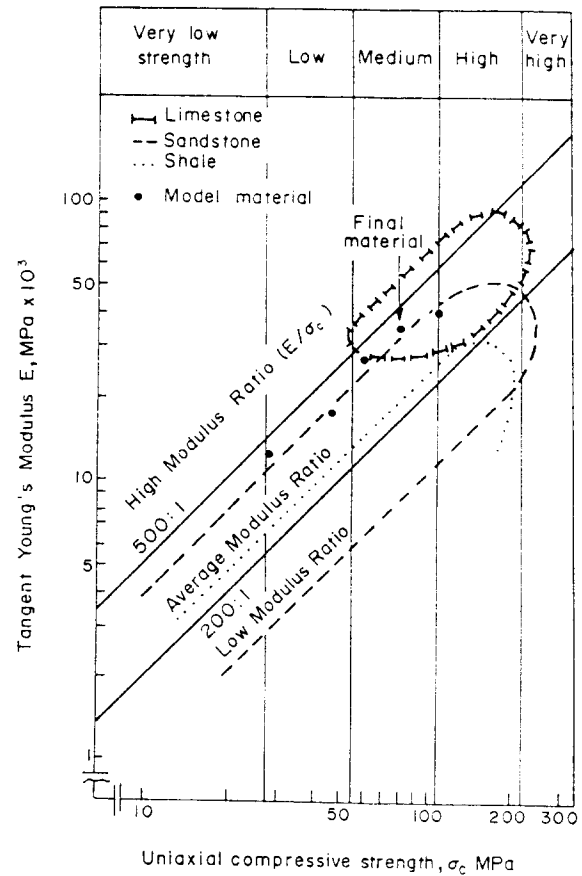

Fig. 3. Relative position of the model materials in Deere and Millers system of intact rock classification. The rock envelopes were taken from Deere [16].

The angle of basic friction (ϕ_b) of the model material was measured in residual shear tests conducted on perfectly flat model surfaces. The residual $\tau - \sigma_n$ envelope was linear within the range of normal stresses from 7×10^{-3} to 0.1 MPa (approximately 0.30-4.0 MPa at prototype scale) and ϕ_b was 32°, which is within the range of 30°-35° often found for unweathered sandstone and limestone rock types.

GENERAL SHEAR CHARACTERISTICS OF MODEL JOINTS

Prior to initiation of the main testing programme, a preliminary investigation was conducted to compare the shear behaviour of the model joints with that expected from real rock joints. A number of identical replicas were cast from rubber moulds of four natural joint samples (9 × 5 cm) with distinctly different surface roughness, as seen in Fig. 4. The uniaxial compression strength (σ_c) of the model material was 2.0 MPa (= 80 MPa prototype rock). Identical replicas of each joint type were sheared under σ_n ranging from 1×10^{-3} to 0.10 MPa (0.04-4.0 MPa at prototype scale) and the results are summarized in Figs 4-7.

Typical examples of the shear stress (τ)-displacement (d_h) relationships under different levels of normal stress (σ_n) are shown in Fig. 4. The diagrams illustrate the anticipated effects of roughness on peak shear strength and stiffness at all levels of normal stress. The joint
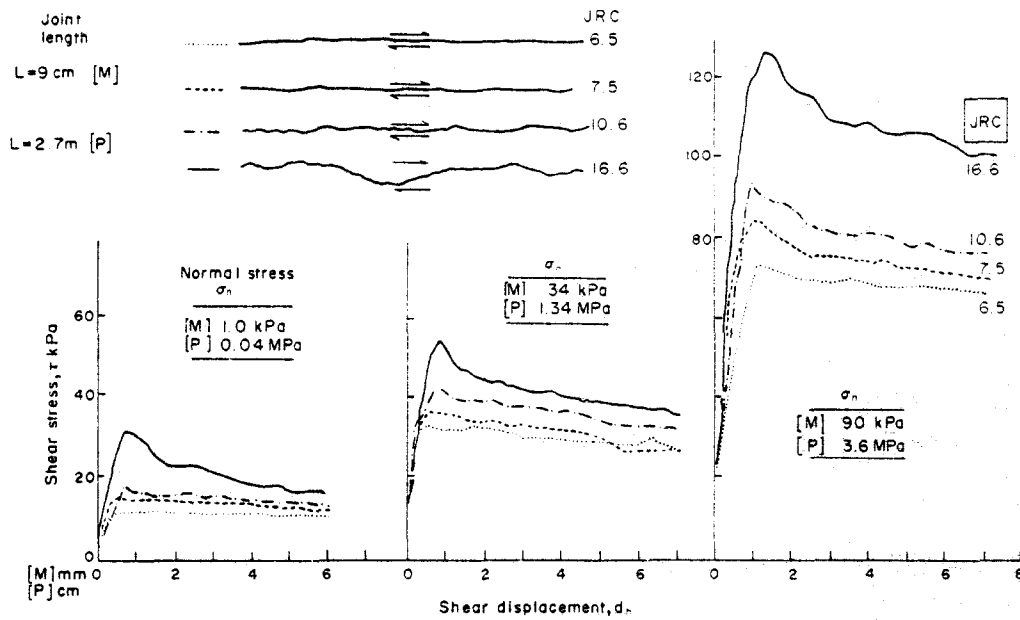
Fig. 4. Shear stress—shear displacement behaviour of model joints with different surface roughness, tested under three levels of normal stress. [M] = model, [P] = prototype.

roughness coefficient (JRC) values assigned to each joint type in Fig. 4 were back-calculated from Barton's [17] empirical equation for peak shear strength (τ_p):

$$\tau_p = \sigma_n \tan\left[JRC \log_{10}\left(\frac{JCS}{\sigma_n}\right) + \phi_r \right] \quad (2)$$

where

σ_n = normal stress

JRC = joint roughness coefficient

JCS = joint compression strength (equal to σ_c here)

ϕ_r = residual angle of friction (equal to ϕ_b here)

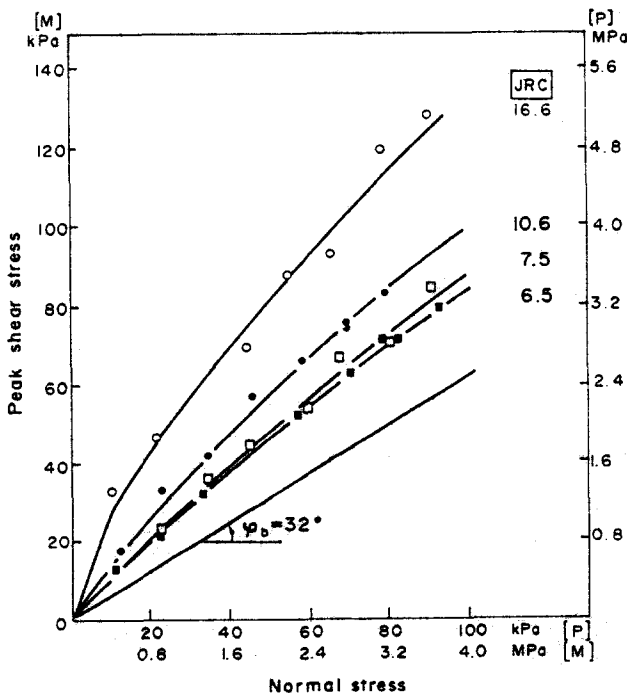Equation (2) gives a good fit to the experimental data of all four model joint types. Figure 5 shows that the peak shear strength of the model joints changes in the fashion expected for real rock joints over a wide range of normal stress. It is also interesting to note the realistic changes in the dilation characteristics with changing JRC (Fig. 6) and the variations in the peak dilation angle (d_n^o) with increasing σ_n and JRC (Fig. 7).

Barton & Choubey [12] have shown that JRC can be considered as a constant irrespective of the level of normal stress (σ_n) within the range of engineering interest. This has also been confirmed by the present model joint test results. However, indications are that the value of JRC may change with increasing length of joint. The other significant input parameter in equation (2) is the joint compression strength (JCS). The effects of JCS on peak shear strength (τ_p) are illustrated in Fig. 8 for three different values of JRC. If JCS is also scale dependent then the envelopes in Fig. 8 imply that the scale effect on τ_p would be maximum for joints of high JRC and minimum for joints of low JRC.
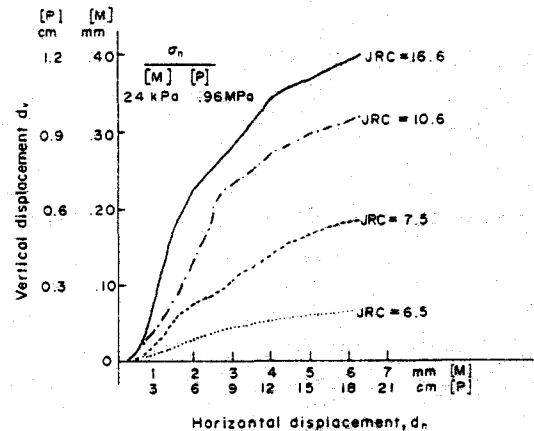

Fig. 5. Peak strength envelopes for the four sets of model joints. Curves were fitted using Barton's [17] empirical equation.

Fig. 6. Model joints demonstrate the effect of surface roughness (JRC) on the dilation.
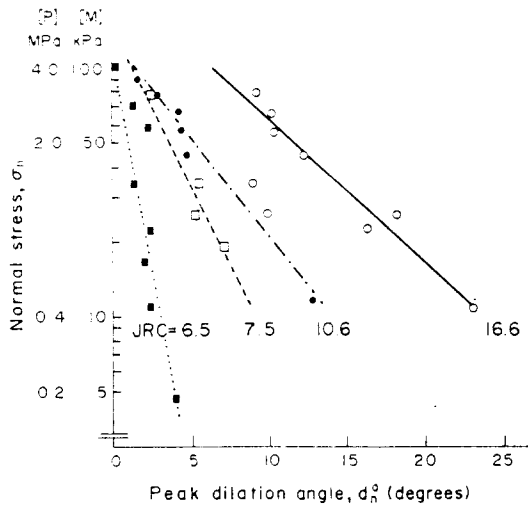
Fig. 7. Effect of normal stress on the peak dilation angle.

DESCRIPTION OF JOINT TYPES

A total of eleven natural joint samples were finally selected for the scale effect investigation. Surfaces ranged from rough undulating to almost smooth and planar. The joint samples were collected from natural exposures of coarse grained sandstone, siltstone, limestone and a lightly metamorphosed fine grained sandstone. The genetic type of those joints ranges from tension and shear joints to bedding planes. A selection of typical longitudinal profiles is illustrated in Fig. 9.

Technical details of the preparation of the moulds and model joint replicas are described by Bandis [14].

The initial study of the fundamental shear characteristics of the model joints reveals realistic behaviour at least from a qualitative standpoint. However, it is necessary to consider the quantitative relation between the model joints and the rock joints, based on the laws of model-prototype simulation. The various sized model samples represent full scale joint lengths of 1.5–1.8 m, 3.0–3.6 m, 5.4–6.0 m or 10.8–12.0 m (full-size replica). The inherent weakness of modelling joints is that scaling of the model roughness in both the normal and tangential directions may lead to an exaggerated surface geometry in relation to the length of joint. The use of a relatively small geometric scale factor ($\lambda = 30$) has probably kept this exaggeration effect to reasonable levels, at least for the majority of the present joint types. For example the full scale wavelengths (1–3 m) and amplitudes (12–20 cm) of the protrusions on the most irregular surfaces (e.g. Nos 1–3 in Fig. 9) compare favourably with similar data from the literature (e.g. Motilevskaya [18]) although it is difficult to assess how realistic is the overall roughness in relation to the length of joint. The most reaslistic 'prototype' roughness is probably that of joint types such as Nos 7–11 where vertical amplitudes were no more than 5–10 cm over the simulated lengths of 10.8–12.0 m.

EXPERIMENTAL RESULTS

The smallest (subdivided) joint replicas were tested in a Wykeham Farrance WF 25300 soils shear box, and
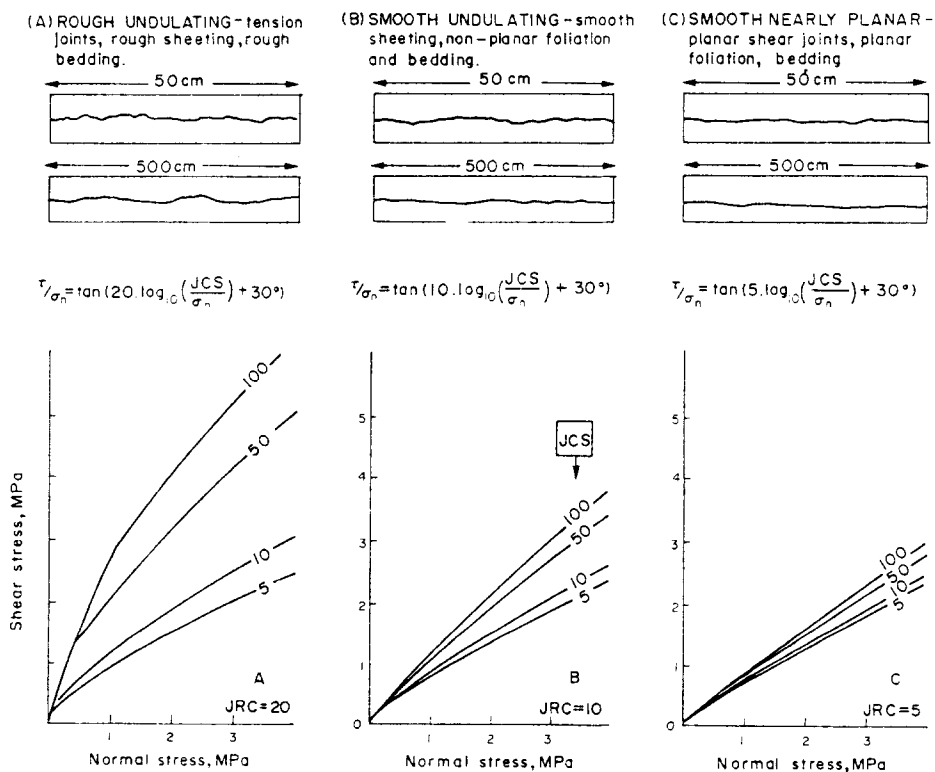

Fig. 8. Illustration of Barton's empirical law of friction in graphical form. Each curve is numbered with the appropriate JCS value (MPa units).
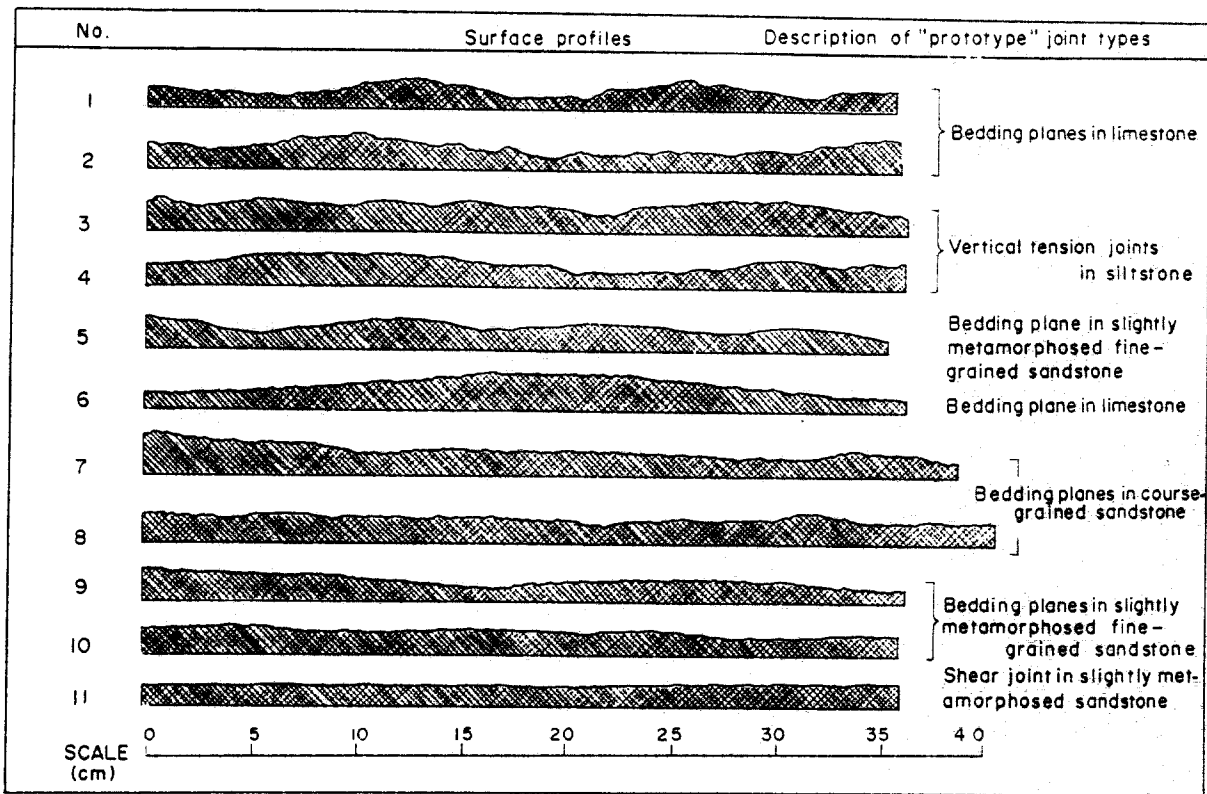
Fig. 9. Selection of typical surface profiles (undistorted) showing the range of joint surfaces investigated.

the larger samples in a specially constructed direct shear apparatus. Caution was exercised to maintain the same horizontal datum during testing of all sample sizes and to apply exactly the same level of normal stress (σ_n). At prototype scale the normal stress was equivalent to approximately 1.0 MPa (i.e. $JCS/\sigma_n \approx 80$). The stringent techniques employed in the preparation of replicas of the same original joint ensured identical interlocking surface roughness. However, increasing block size or length of joint revealed remarkable scale effects on both the shear strength and deformation characteristics.

As an introduction to the magnitude of the scale effect on peak shear strength, an overall summary

of the results is presented in Table 1, where the eleven types of model joints have been broadly divided into three groups according to their roughness. The peak total friction angles (ϕ_p = peak arctan τ/σ_n) are described by the mean and standard deviation values. A comparison shows that the mean ϕ_p value decreases by approximately 8°–20° as the length of individual blocks increases from 5 or 6 cm to 36 or 40 cm (1.5–1.8 m to 10.8–12 m at prototype scale).

Another illustration of this remarkable scale effect is shown in Fig. 10 where the mean peak shear stress $(\bar{\tau}_p)$ of all joint replicas has been plotted against the average joint area (A). It is interesting to note the non-linear scale effect $\bar{\tau}_p$ which evidently tends to an asymptotic

TABLE 1. SUMMARY OF MEAN PEAK ARCTAN (τ/σ_n) VALUES OBTAINED FROM MODEL JOINTS WITH COMPARABLE SURFACE MORPHOLOGY BY VARYING THE AVERAGE JOINT LENGTH

Joint length (L)		Description of joint roughness			
Model (cm)	Prototype (m)	Strongly undulating, rough	Strongly undulating, moderately rough	Moderately undulating, very rough	Moderately undulating to almost planar, moderately rough to almost smooth
[M]	[P]				
Model nos		1, 2, 3	4, 5	6, 7, 8	9, 10, 11
5, 6	1.5, 1.8	64.5° ± 6.8° (54)	58.4° ± 8.3° (36)	64.3° ± 6.3° (74)	49.8° ± 6.4° (54)
10, 12	3.0, 3.6	59.4° ± 7.9° (18)	58.7° ± 5.6° (12)	60.7° ± 6.3° (33)	46.1° ± 6.1° (18)
18, 20	5.4, 6.0	56.2° ± 3.8° (12)	53.4° ± 3.2° (8)	52.1° ± 5.9° (12)	43.0° ± 5.0° (12)
36, 40	10.8, 12.0	51.9° ± 4.1° (3)	48.1° (2)	45.5° ± 1.6° (3)	41.5° ± 2.6° (3)

Notes:
The ± values correspond to one standard deviation.
Numbers in brackets give the corresponding total number of specimens from all joint types in that group.
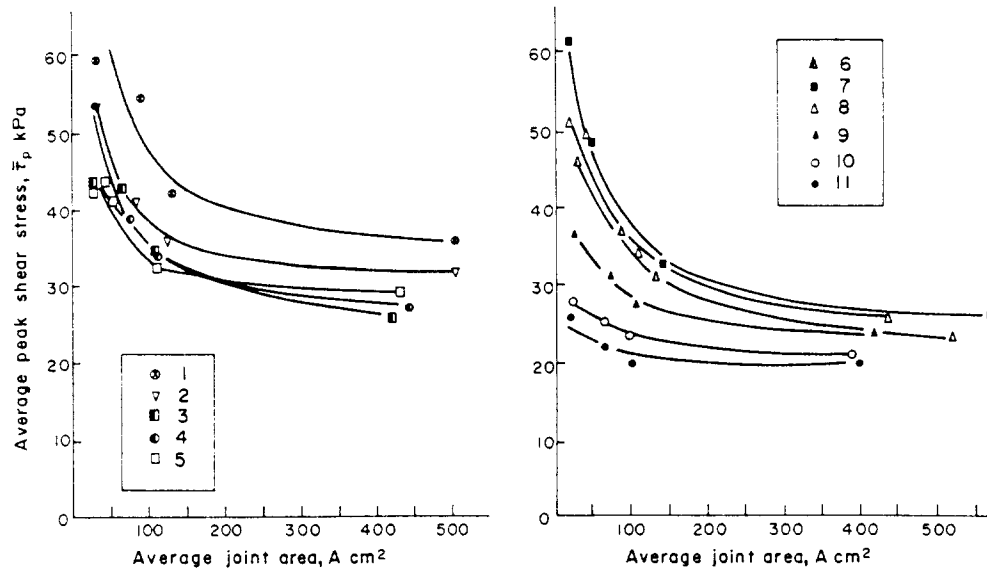
Fig. 10. Variation of average peak shear stress with joint specimen area.

value with increasing A. Similar non-linear trends are also observed in plots of $\bar{\tau}_p$ vs joint length (L) but the 'floor' is less pronounced for the longest joints. The apparent decline of the scale effect with decreasing surface roughness (e.g. see Nos 9, 10 and 11) should also be carefully noted.

The shear stress (τ)-displacement (d_h) relationship illustrated in Figs 11, 12 and 13 are typical examples of the overall scale effect on joint shear behaviour. It is shown that increasing block size or length of joint leads to:

(i) a gradual increase in the peak shear displacement (d_{hp});

(ii) an apparent transition from a 'brittle' to 'plastic' mode of shear failure;

(iii) a decrease of the peak dilation angle d_n° Figs 11(b), 12(b) and 13(b);

(iv) insignificant scale effects in the case of relatively planar and smooth joint types (Fig. 13).

It should be noted that the cumulative mean τ–d_h curves shown in Figs 11, 12 and 13 are derived by averaging the shear forces which acted upon each of the component blocks at regular increments of shear displacement. Similar procedure is followed for the derivation of the cumulative mean dilation curves.

EFFECT OF SCALE ON PEAK SHEAR DISPLACEMENT

The scale effect on peak shear displacement (d_{hp}) is illustrated in Fig. 14 where the mean d_{hp} values from each subdivided model are plotted against the respective joint length (L). The three families of curves indicate that the type of surface roughness has a decisive
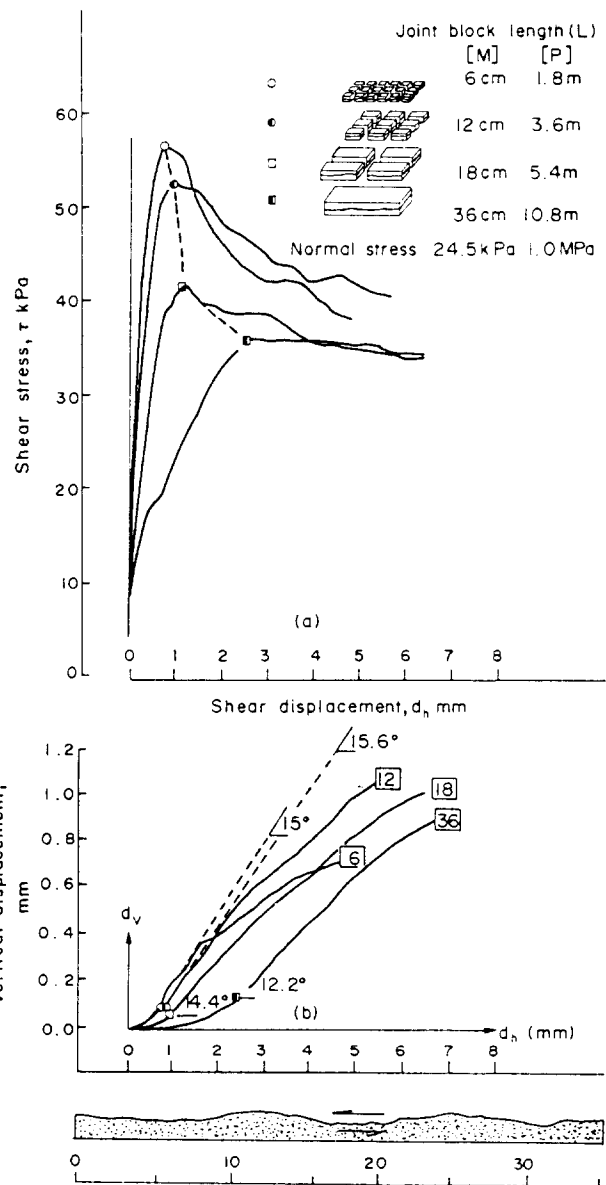

Fig. 11. Cumulative mean shear stress—shear displacement (a) and dilation (b) curves of model No. 1.
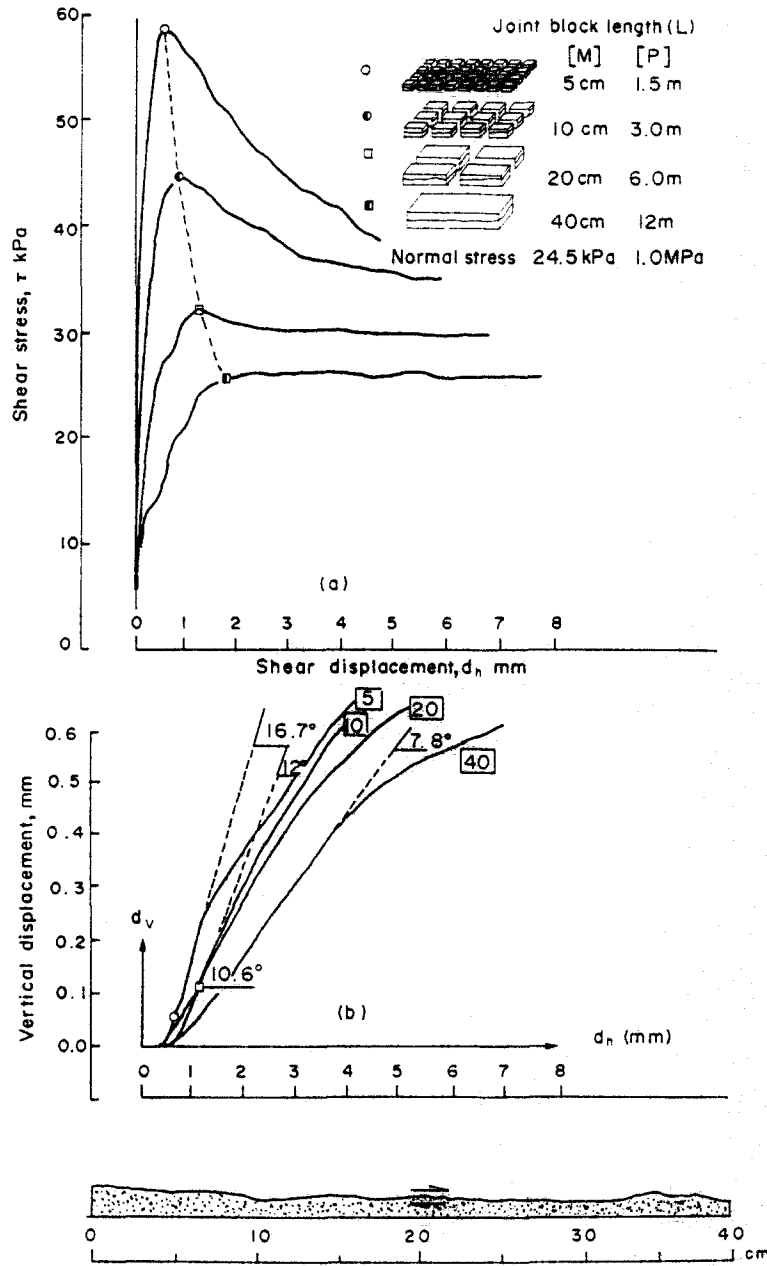
S. Bandis, A. C. Lumsden and N. R. Barton

Fig. 12. Cumulative mean shear stress—shear displacement (a) and dilation (b) curves of model No. 7.

influence on the variation of d_{hp} with increasing block size. Peak shear displacement is effectively a measure of the distance a joint has to travel until effective contact is made between the asperities controlling its peak resistance. The displacement-scale effect clearly implies that under the same level of normal stress the peak behaviour of different joint lengths is controlled by irregularities of different size or base-length.

Indirect evidence of this effect is given by the change in behaviour from 'brittle' to 'plastic' with increasing scale. Such a pattern was found to persist, to a greater or lesser extent, in all the highly irregular types of surfaces tested. It is similarly reasonable to expect that ultimate strength is approached after displacements larger than the size or base-length of those asperities which control the peak behaviour.

EFFECT OF SCALE
PEAK DILATION

Mean dilation curves for the different sizes of joint replicas can be seen in Figs 11(b), 12(b) and 13(b). The peak dilation angles (d_n^o) are calculated from the portion of the dilation curve corresponding to peak shear displacement. The variation of mean d_n^o values with joint length is illustrated in Fig. 15.

The peak dilation angle represents the inclination of the contacts between the 'critical' asperities at the instant of peak strength (relative to the mean joint plane). Analyses of joint profiles have shown that the longer the base-length considered, the less steep the asperities [19–21]. By considering the scale effect on both peak shear displacement (d_{hp}) and peak dilation
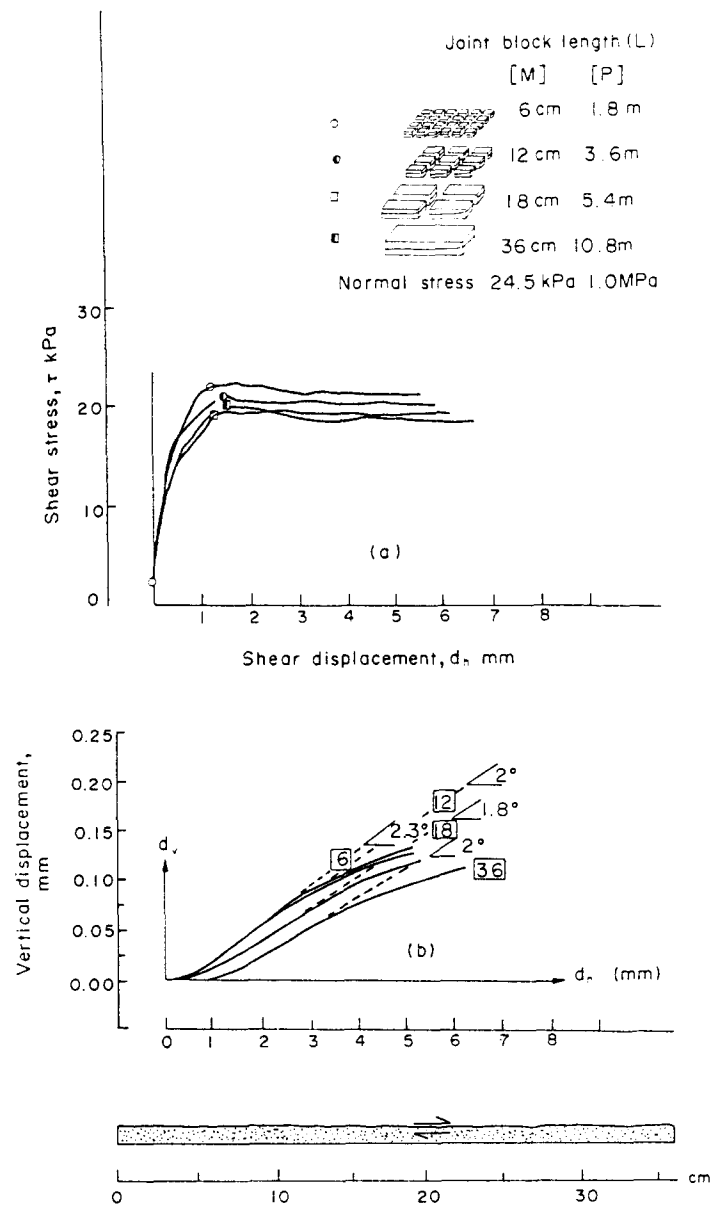
Fig. 13. Cumulative mean shear stress—shear displacement (a) and dilation (b) curves of model No. 11.
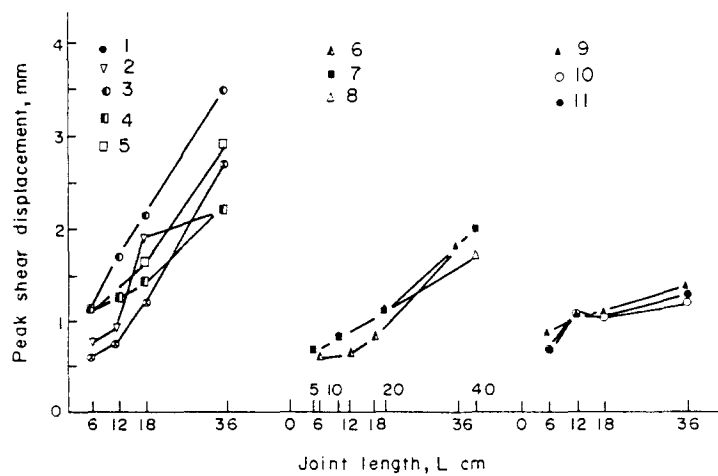
Fig. 14. Variation of peak shear displacement with increasing length of joint specimen.
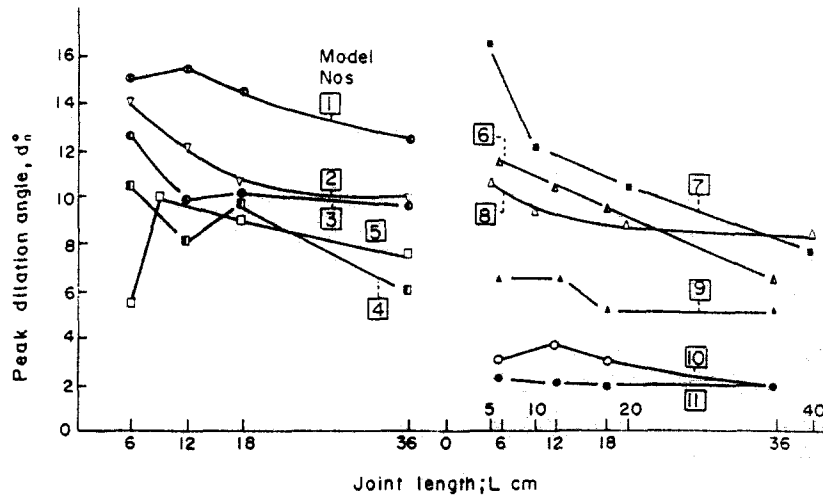
Fig. 15. Variation of peak dilation angles with increasing length of joint specimen.

(d_n°) it becomes clear that as the length of the joint blocks increases, peak resistance is not reached until effective contacts have developed between asperities of longer base-length and correspondingly flatter slopes. This is confirmed from post-test observations of the sheared surfaces, as will be discussed later.

EFFECT ON SCALE ON JRC

The mobilization of asperities of different baselength means that the value of the joint roughness coefficient (JRC) for a particular joint or joint set will depend on scale. A joint with small steep asperities controlling peak behaviour would have a higher JRC value than a longer profile of the same joint whose behaviour was dominated by larger and less steeply inclined surface features.

The relationships between mean JRC values (back-calculated from equation 2) and joint length (L) are illustrated in Fig. 16. It is shown that the JRC values reduced by a maximum of 1.3 (for planar joints) and by

a maximum of 11.2 (for rough joints). As will be discussed later, indications are that the joint compression strength (JCS) is also scale-dependent. The scale effect on JRC seen in Fig. 16 may therefore be exaggerated, since a constant JCS value of 2.0 MPa (equal to the compression strength σ_c of the model material) has been assumed in calculations up to this point.

EFFECT OF SCALE ON ASPERITY FAILURE COMPONENT

The reduction in the peak dilation angle (d_n°) with increasing joint size (Fig. 15) accounts for part of the scale effect on the peak friction angle (ϕ_p). Under a given σ_n, complete or partial damage of asperities contribute a shearing or failure component (S_A°) to the peak frictional resistance (ϕ_p) which is represented by

$$\phi_p^\circ = \text{peak arctan} (\tau/\sigma_n)^\circ = \phi_b^\circ + d_n^\circ + S_A^\circ \qquad (3)$$

as indicated diagrammatically in Fig. 17. Had d_n° been the only scale dependent parameter, one would expect
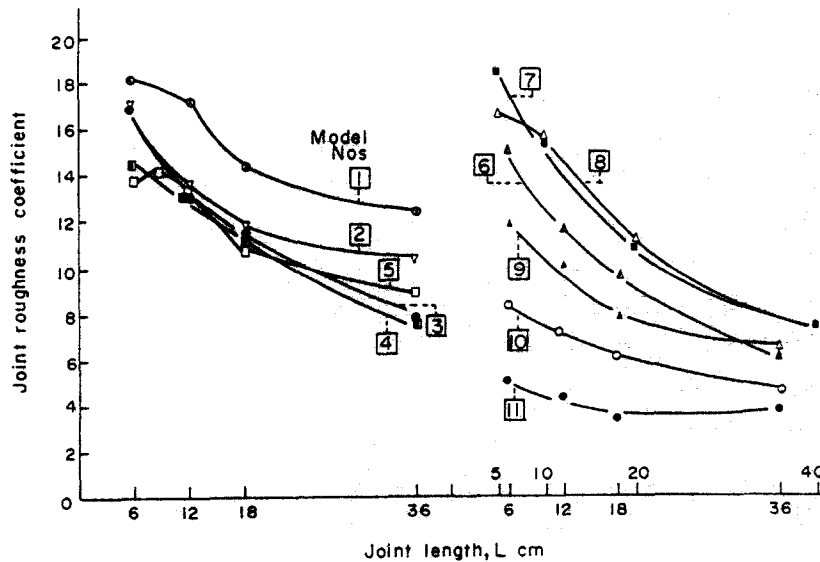

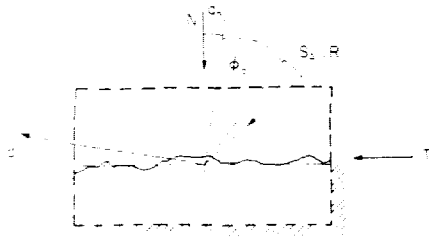Fig. 16. Apparent variation of JRC with increasing length of joint specimen.

Fig. 17. The angular components of shear strength for an undulating joint, after Barton [17].

the peak asperity failure component (S_A) to remain unchanged with increasing length of joint since ϕ_b is constant. However, the mean values of S_A estimated from:

$$S_A = \phi_p - (\phi_b' + d_n')$$

reveal a strong scale effect as shown by the data in Table 2.

EFFECT OF SCALE ON THE SIZE AND DISTRIBUTION OF CONTACT AREAS

The smallest joint replicas (5–6 cm long) were sheared a total of 5–6 mm ($d_h/L \approx 10\%$) while the corresponding full size joints (36–40 cm long) were sheared 6–8 mm ($d_h/L \approx 1.8\%$). The different relative amounts of post-peak shearing make quantitative comparison of post-test contact areas of questionable value. However, visual comparison of the post-test contact areas shown in Figs 18 and 19 reveals the following basic features:

(i) an increased number of small contact areas on the small samples;

(ii) an increased size of individual contact areas on the large samples;

(iii) both these scale effects are reduced for the case of planar joints.

TABLE 2. VARIATION OF THE MEAN ASPERITY FAILURE COMPONENT (S_A) WITH INCREASING JOINT LENGTH (L)

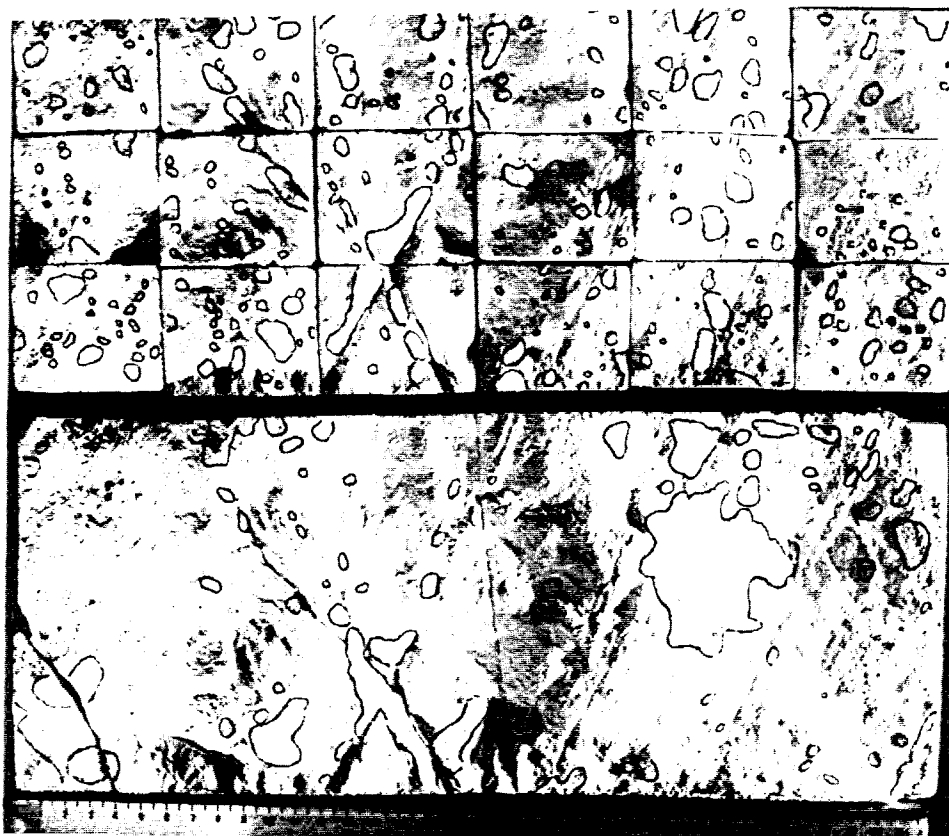| Joint length (L) | | | | | | Models nos | | | | | |
Model (cm)	Prototype (m)	1	2	3	4	5	6	7	8	9	10	11
5, 6	1.5, 1.8	19.6	18.1	19.9	17.3	21.1	17.3	18.7	19.5	16.3	13.1	7.5
10, 12	3.0, 3.6	17.4	14.2	15.4	16.8	17.1	12.2	17.2	17.9	12.7	9.6	6.6
18, 20	5.4, 6.0	13.2	12.4	12.2	12.1	12.1	8.7	10.4	12.1	10.7	8.3	4.9
36, 40	10.8, 12.0	11.7	10.1	5.3	8.4	10.3	5.1	6.2	6.0	7.3	6.6	5.3

Fig. 18. Photograph illustrating the distribution, number, and size of post-test contact areas on small and large joint samples of model No. 1.
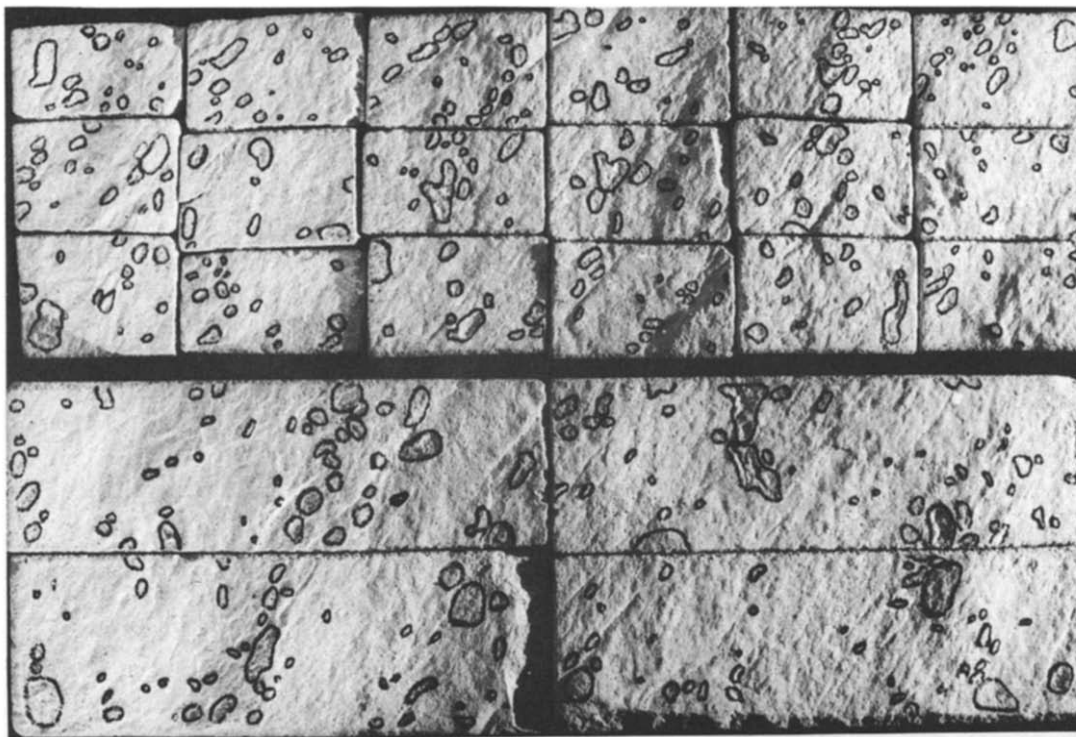
Fig. 19. Photograph illustrating the distribution, number and size of post-test contact areas on small and large joint samples of model No. 11.

Noting that post-peak wear of the asperities must be least for the case of the largest samples, it is nevertheless these large samples which mobilize the largest asperities. This is a fundamental feature of joint shearing, and explains several aspects of the scale effect.

In the case of the rough undulating joint (Fig. 18) the mean asperity failure component (S_A°) is estimated for the 6 cm samples as $\simeq 8^\circ$ higher than the S_A° value of the 36 cm long joint. In the case of the planar joint (Fig. 19) the mean S_A° value drops by only 2.6° as the block size increases from 6 to 18 cm, and significantly the difference in the size of the individual contacts on both sample sizes is very small. It seems, therefore, that the increasing size of the individual areas of contact is part of a mechanism which causes the significant reductions in the asperity failure component at larger scale.

Barton [13], and Barton & Choubey [12] have previously discussed the likelihood of a scale effect on the joint compression strength (JCS). It is known from numerous tests that the intrinsic strength of rock materials is inversely related to specimen size [22, 23]. Consequently, it is reasonable to assume that the large irregularities mobilized during shear of large samples will resist lower stresses than the small asperities mobilized during shear of small samples.

Lama and Gonano's review of scale effects on uniaxial compression strength indicate that most of the strength reduction occurs in the size range $1.0-10^4$ cm^3. The existence of an approximate 'cut-off' at 10 l, corresponding to perhaps 25×25 cm^2 sample cross-sections, suggests that this JCS scale effect will also die out with increasing length of joint samples. Possibly

joints of several metres length will mobilize contact areas of this order of magnitude.

Size-effects in the uniaxial compression strength (σ_c) of plaster/sand based model materials have also been reported in the past (e.g. [22, 24] and it is likely that a similar effect existed in the present material. The scale effect on JCS ($=\sigma_c$) explains the reduced asperity failure component of longer joints. It now remains to determine by how much JCS can be expected to reduce with increasing joint size.

Reduction factors for JCS are derived from the ratios of S_A° corresponding to the 5–6 cm long samples and those obtained from the longer joints. A complete picture of the magnitude of the scale effect on JCS is presented in Fig. 20. The scatter in the JCS values of the long joint samples is significant and occurs because of the different size of individual contacts, which generally decrease with increasing joint planarity. Use of the scale-reduced JCS in equation (2) gives higher JRC values than those in Fig. 16 where a constant JCS is assumed. The relationships in Fig. 21 give a more realistic picture of the magnitude of the scale effect on JRC.

It is important to note that despite the large reduction in the JRC of non-planar joints and the small reductions in the JRC of planar joints there is nevertheless no complete convergence to a narrow range of JRC values at large scale. Joints apparently retain their individual character at all scales, even though they are more alike as dimensions increase. The present variety of surface roughness represents a JRC range of 5–18.5 in the 5–6 cm samples (= 1.5–1.8 m at prototype scale),
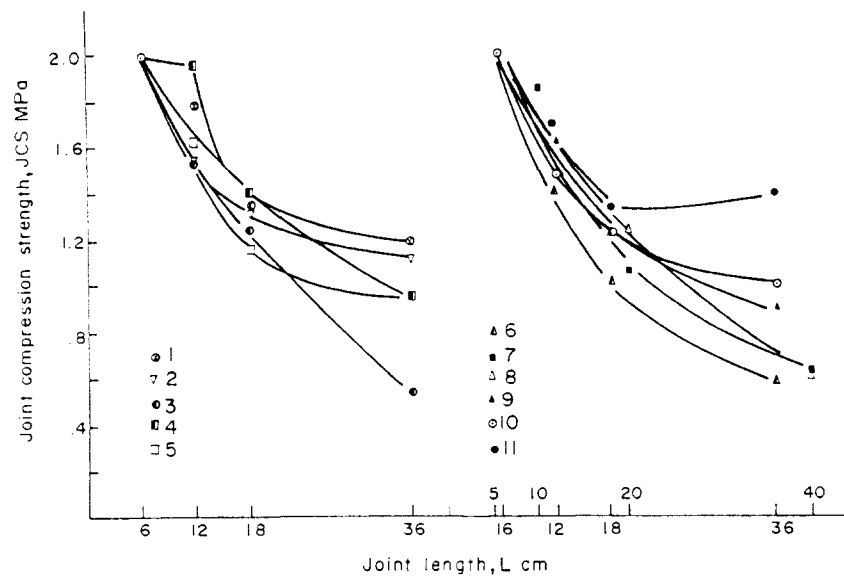
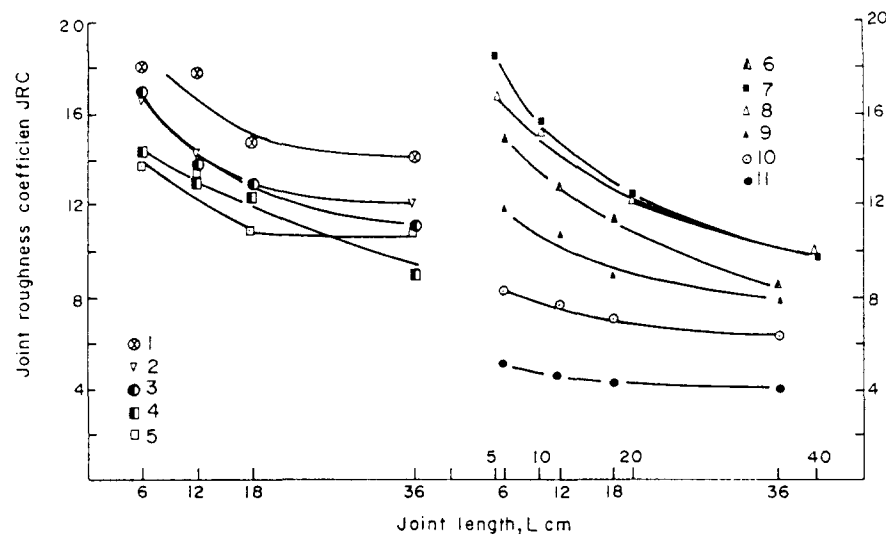Fig. 20. Effect of scale on joint wall compression strength (JCS).

Fig. 21. Effect of scale on the joint roughness coefficient (JRC). Values of JRC were back-calculated from equation (2) using the scale-corrected values of JCS.

reducing to 4–14 in the 36–40 cm samples (= 10.8–12.0 m long prototype joints). This signifies that surfaces roughness represents a fundamental component of shear strength at any scale. Figure 22 summarizes the present scale effects in dimensionless form. It appears that prediction of the approximate magnitude of scale effects is possible once JRC_0 (from 'laboratory' size samples) is known.

SCALE EFFECT AT DIFFERENT LEVELS OF NORMAL STRESS

A series of tests was conducted on a complete set of sample sizes of the rough, undulating joint no. 2 under normal stresses (σ_n) up to 61.25 kPa, = 2.45 MPa at prototype scale. A summary of the results is presented in Fig. 23. It is shown that the scale effect on ϕ_p decreases with increasing normal stress. This is because both the peak dilation angle d_n° and the asperity com-

ponent S_A° of the small samples decrease by a relatively larger amount than in the case of the full-size joint. This can be explained by the relative effects of normal stress on contact areas. As the normal stress increases the contact areas on the 6 cm samples increases and the effective JCS decreases, hence the reduction in S_A°. An analogous increase of the contact areas on the 36 cm joint under the same σ_n does not cause significant change in the value of JCS, which has already approached its scale effect limit as shown by the asymptotic relationship in Fig. 22, and hence the virtually identical values of S_A°. For the same reason the peak dilation angle (d_n°) shows a relatively smaller reduction under higher σ_n as the joint length increases.

The agreement between the theoretical peak shear strength envelopes and the experimental data is shown in Fig. 24. As can be seen, both JRC and JCS have been correctly scale-reduced with increasing sample size. A summary of the above scale effects is shown in Fig. 25.
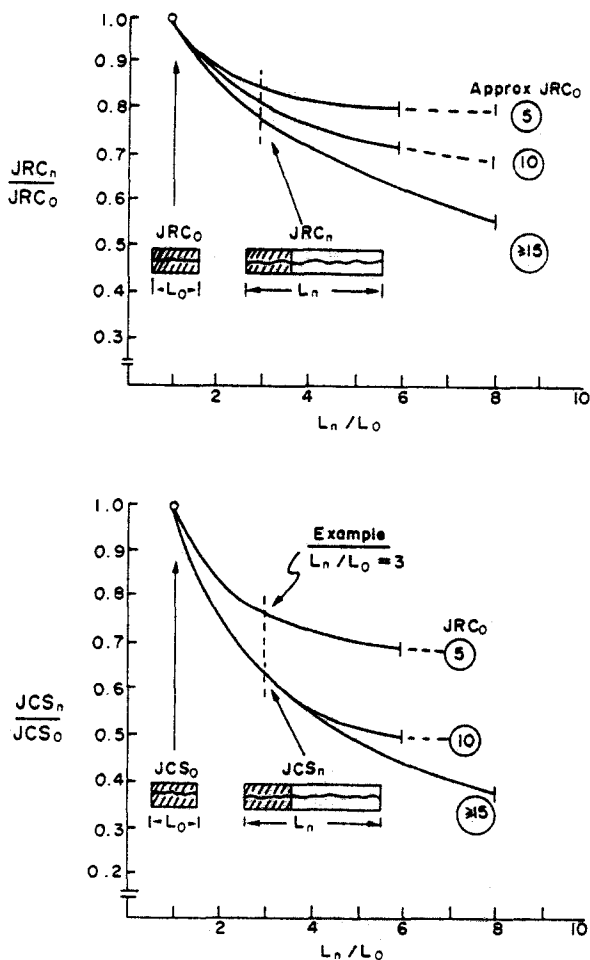
Fig. 22. Experimental scale effects in dimensionless form.

Fig. 24. Theoretical envelopes fitted to experimental data, using scale-reduced values of JRC and JCS to account for the increasing lengths of samples.

The four columns indicate diagrammatically how the components S_A° and d_n° reduce with increasing scale. The asperity failure component reduces relatively more than the dilation (geometrical) component.
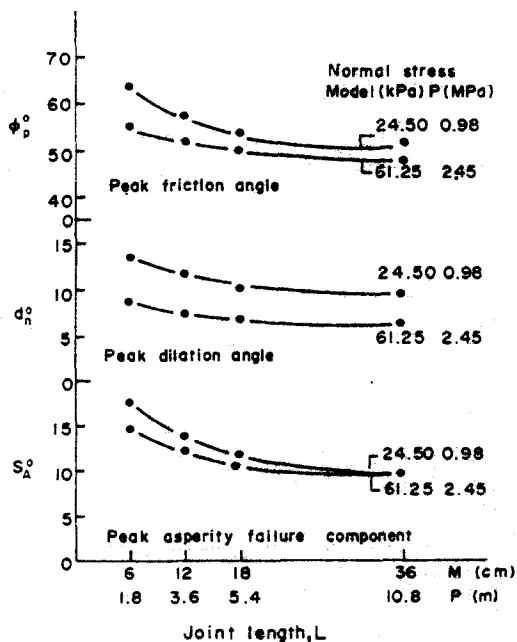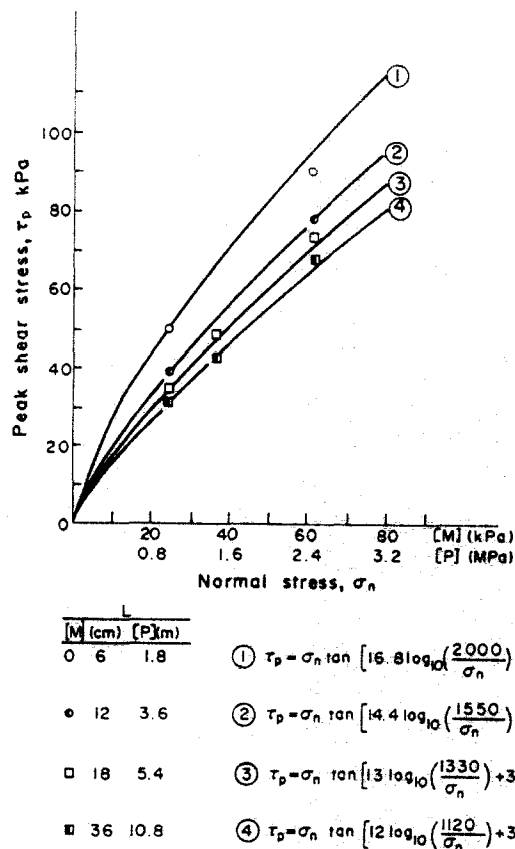

Fig. 23. Various effects of scale at different levels of normal stress.

Size limit for d_h (peak)

On the basis of results from shear tests on model tension fractures [25] and later, tests on 10 cm long rock joints, Barton & Choubey [12] suggested as a simple 'rule-of-thumb' that d_{hp} is reached after a shear displacement equal to $\simeq 1\%$ of the joint sample length (L) up to some limiting size (L_c). This rule-of-thumb is tested against the present data and the findings are summarized in Table 3.

As indicated, the empirical rule shows good agreement, with the exception of the large samples (18–40 cm) of joint nos 6–11. Barton & Choubey [12] noted that d_{hp} should be expected to reduce below 1% of the joint length as the latter increased to several meters. Defining a limit of validity for the '1%' rule is complicated by the effects of roughness on the peak displacement. The present data indicate a limiting length of about 5 m for undulating joints and 3 m for joints with less wavy to planar surfaces.

Progressive failure of asperities

A quite common feature of the pre-peak portion of a number of τ-d_h curves representing large joints (18–40 cm in length) is the occurrence of one or more inflection points followed by discernible decrease in slope, as indicated by the idealized diagrams in Fig. 25. Since the model joints were fully interlocked prior to application of the shear force, it is probable that the

TABLE 3. SUMMARY OF EXPERIMENTAL PEAK SHEAR DISPLACEMENT (d_{hp}) DATA IN RELATION
TO JOINT LENGTH (L)

Joint length (L)		$\dfrac{\text{Mean } d_{hp}}{\text{Joint length } (L)} \times 100$		
Model (cm)	Prototype (m)	1, 2, 3, 4, 5	6, 7, 8	9, 10, 11
5, 6	1.5, 1.8	1.5%	1.2%	1.2%
10, 12	3.0, 3.6	1.0%	0.7%	0.9%
18, 20	5.4, 6.0	0.9%	0.5%	0.6%
36, 40	10.8, 12.0	0.7%	0.5%	0.4%

changing shape of the curves with increasing scale is the result of 'progressive' failure of asperities along the longer joints. It is envisaged that during the course of pre-peak-deformation, a joint will have to overcome the 'interference' of asperities of smaller size than the critical asperities for the particular length. Notably, the changes in slope often occur after displacements roughly equal to the peak displacements (d_{hp}) of the 6 cm and or 12 cm long joints.

Scale effect on ultimate strength

The τ–d_h diagrams in Fig. 25 also summarize the scale effect on the post-peak behaviour. It is shown that as the joint length decreases, larger relative shear displacement is needed for the ultimate strength (τ_{ult}) to be reached. Experimental results showing these features are seen in Figs 11, 12 and 13. This emphasizes an additional problem of design based on laboratory size joint samples. The ultimate strength measured in small shear boxes is higher than that which would be measured on a large exposure of the same joint. Thus not only peak but also 'ultimate' strength is scale dependent. True residual strength cannot be reached until much larger displacements have occurred. For this reason it is useful to have a conservative empirical method of estimating ϕ_r (see later).

Multiply-jointed rock

An inherent limitation in direct shear testing of individual jointed blocks is that the response of the surrounding rock mass is absent. This may sometimes lead to erroneous extrapolations. For example, the joints studied show a transition from 'brittle' to 'plastic' behaviour as the scale increases. This is an important feature of individual joint behaviour. Nevertheless, the much larger number of blocks in a heavily jointed rock mass would tend to cause more 'plastic' collective behaviour. (Joint roughness might also be less marked in such cases, further emphasising the 'plastic' behaviour).

The results from this study indicate that the peak shear strength of a closely jointed rock mass (with given joint roughness) should be higher than for a rock mass with wider joint spacing. The question is whether the stiffness of the rock mass overlying and underlying the plane or zone of shear failure would allow the small blocks to follow the individual shear paths required to maintain contact with their small steep asperities, and thus develop their potentially higher peak shear strength.

Tilt tests conducted on subdivided and full-size models of some of the present types of joints show that the angle of tilt at which failure occurs increases significantly as the joint block size decreases. This is indicated in the sketch in Fig. 26, which is traced from a photograph of one of the multiple-block tilt tests. The different normal stress in the two cases is insufficient to explain the 15° difference in shear strength. Similar tests by Barton & Choubey [12] using natural rock joints also indicated large differences in ϕ_p.

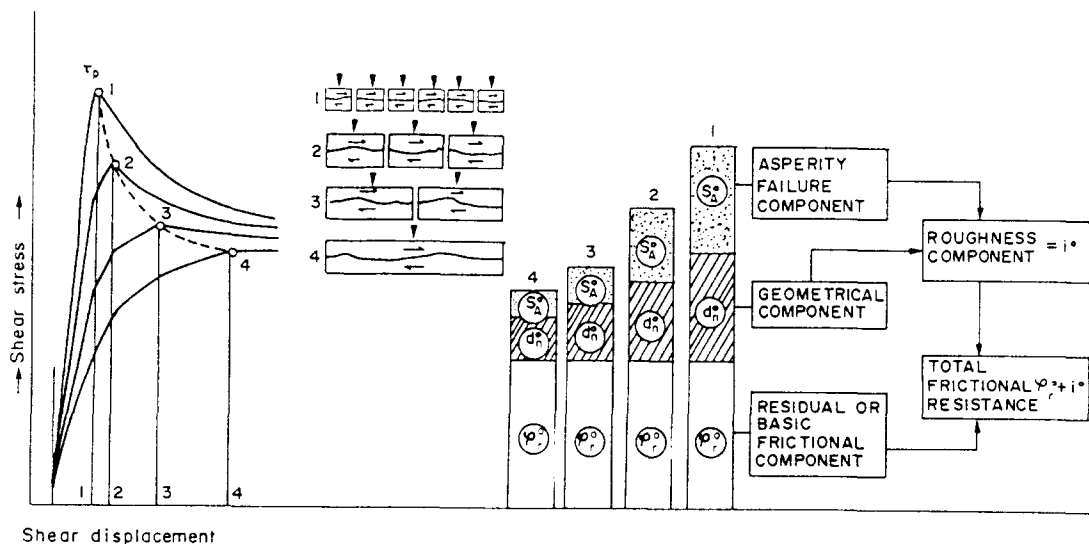In order to study the scale effect in rock masses

Fig. 25. The three shear strength components are affected by sample size in varying degrees.
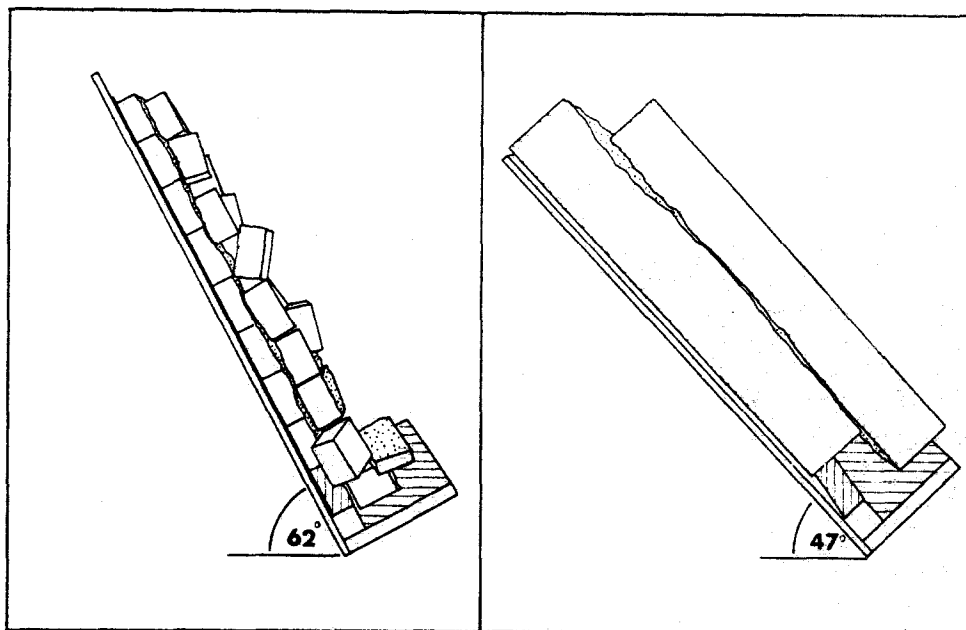
Fig. 26. Tilt tests with multiple blocks indicate higher strength than with large single blocks.

under stress, jointed models simulating different cross-joint spacings were stressed to failure in a simple 40 × 40 cm biaxial frame. 'Primary' and 'secondary' sets of joints were developed using a double-bladed guillotine [25]. Details of the geometry of the model tests are shown in Fig. 27.

It is seen that the model with the most widely spaced joints (L_p = 12.3 m) requires the least shear stress to reach failure, while the most closely jointed model

(L_p = 3.3 m) needs the highest stress. Notably, all three models fail at higher shear stress than the individually tested fractures simulating prototype joints 18 and 30 m long. All the model joints were created in the same manner and had identical roughness. The scale effect on the JRC-values back-calculated from the failure stresses σ_1 and σ_2 are shown in Table 4.

An example of a 'failed' model rock mass is shown in Fig. 28. This was a special test on a model with the
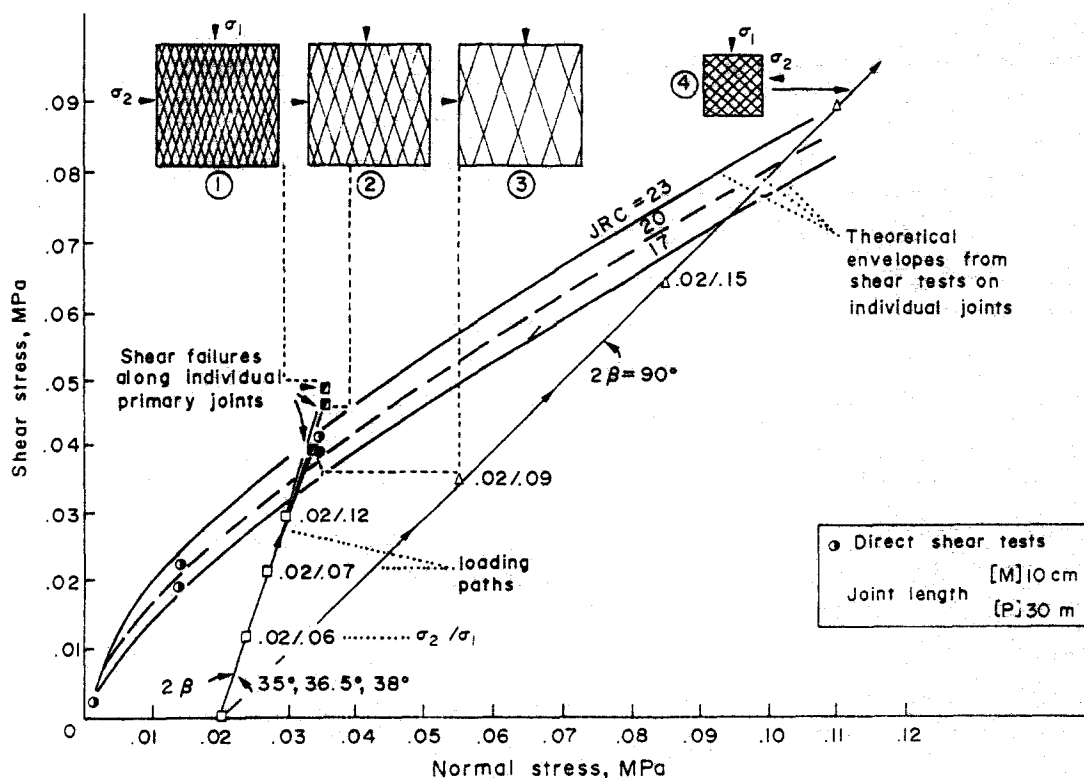

Fig. 27. Biaxial shear tests on jointed models with 4000, 1000 or 250 blocks each. Shear strength is highest with the smallest block sizes.

TABLE 4. EFFECT OF JOINT LENGTH OR CROSS JOINT SPACING ON THE VALUE OF JRC BACK-CALCULATED FROM DIRECT SHEAR AND BIAXIAL TESTS

Type of test		Joint length or cross joint spacing		Joint roughness coefficient (JRC)
		Model scale (mm)	Prototype scale (m)	
Direct shear tests on individual jointed blocks		100	30	Mean of
				> 100
		60	15	tests
Biaxial tests on jointed models		41 (250 blocks)	12.3	21.6
	$\beta = 18$	21 (1000 blocks)	6.4	25.1
		11 (4000 blocks)	3.3	26.7
	$\beta = 45$	6.2 (4000 blocks)	1.8	> 26 (failure did not occur)

same geometry (and loading path) as model 4. However, just before shear failure a 'tunnel' was excavated to reduce the shear resistance locally. Intersecting kink bands occurred suddenly when the simulated tunnel was about 5 m in span.

The well-defined scale effect on the peak shear strength of these jointed model rock masses is related to the changing stiffness of the mass as the joint block size or joint spacing increases or decreases. Densely jointed masses have lower stiffness than widely jointed masses. The effective modulus of deformation (E) of the masses in Fig. 26 decreases from approximately 18.5×10^3 MPa to 7.5×10^3 MPa as the number of blocks increases from approximately 250 ($L_p = 12.3$ m) to 4000 ($L_p = 3.3$ m).

The reduced stiffness of the densely jointed model increases the degree of freedom of the individual joint blocks and enables them to rotate and 'feel' all scales of roughness more readily. Consequently, the small blocks in a densely jointed mass may be able to mobilize higher JRC values than larger blocks in a mass with wider-spaced jointing.
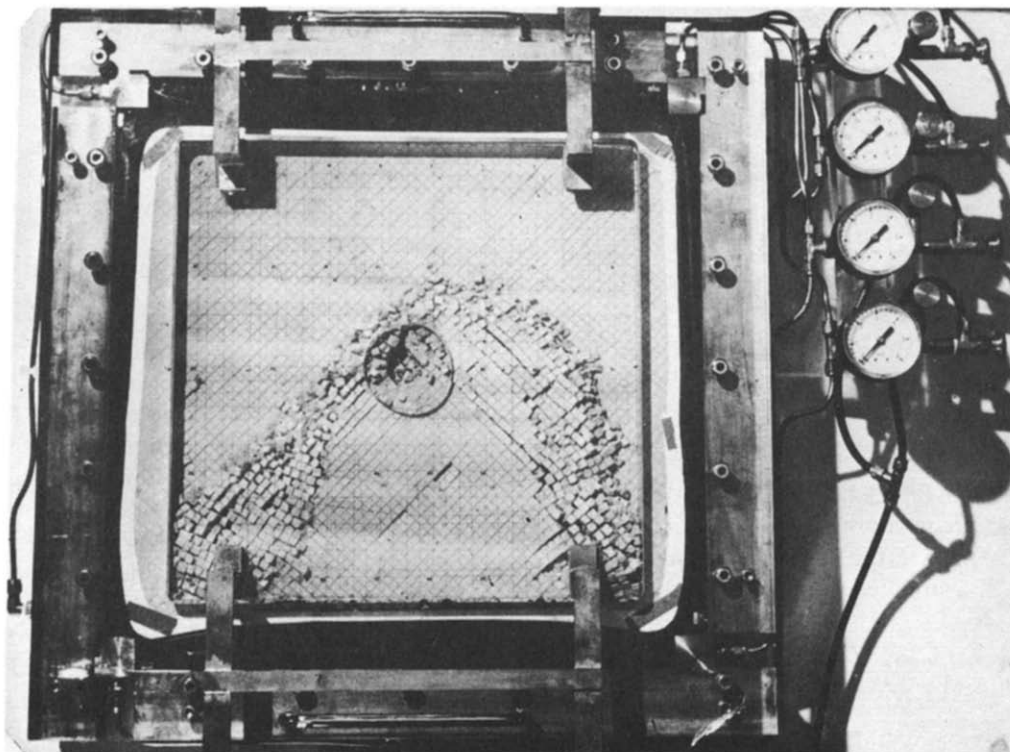

Fig. 28. Failure of a highly stressed model consisting of 4000 blocks is caused by "tunnelling".

PRACTICAL SOLUTIONS TO THE SCALE EFFECT PROBLEM

The scale effect on peak shear strength implies that there is a minimum test specimen size which should be regarded as technically acceptable. Barton & Choubey [12] suggested that the correct joint test size might, as a first approximation, be given by the natural block size, or more specifically, the spacing of cross-joints. The contact faces between the natural blocks probably can be regarded as potential hinges (albeit stiff-ones) preventing significant scale effects for assemblies of blocks. Samples consisting of single (smaller) blocks contain no 'hinges', are stiff and inflexible, and hence experience a scale effect. Beyond the natural block size, scale effects seem less likely, and they would better be accounted for as a change of dip. Of course, in close, randomly-jointed rock masses, undisturbed interlocked multi-block samples may have to be tested in large triaxial cylinders for the correct rock mass strength to be obtained.

In typical cases with wider joint spacing, where it would be impossible to sample multi-block specimens, it should be sufficient to test single blocks of natural size.

Measurements of JRC from large scale index tests

The cheapest solution for obtaining a scale-free estimate of JRC is to conduct simple tilt, pull or push tests on naturally occuring blocks using only the self-weight of the overlying block as the source of normal stress.

Individual blocks with through-going joints can be slowly tilted up to the point (angle α) when sliding occurs down the joint plane. The individual values of JRC can be back-analyzed from each test using equation (2):

$$\text{JRC} = \frac{\alpha^0 - \phi_r}{\log_{10}\left(\dfrac{\text{JCS}}{\sigma_{no}}\right)} \tag{3}$$

where

α = tilt angle

σ_{no} = normal stress when sliding occurs

A diagrammatic illustration of this simple test is given in Fig. 29. The example below shows some typical values.

$\alpha = 51°$ (tilt angle)

$h = 0.50$ m (block height) $\sigma_n \simeq 0.005$ MPa

$\gamma = 25$ kN/m^3 (unit weight)

JCS = 50 MPa (estimated using Schmidt hammer)

$\phi_r = 23°$ (estimated from equation 4)

$$\text{JRC} = \frac{51° - 23°}{\log_{10}\left(\dfrac{50}{0.005}\right)} = 7.0$$

The other two unknowns in equation (3) are the joint compression strength (JCS) and the residual friction
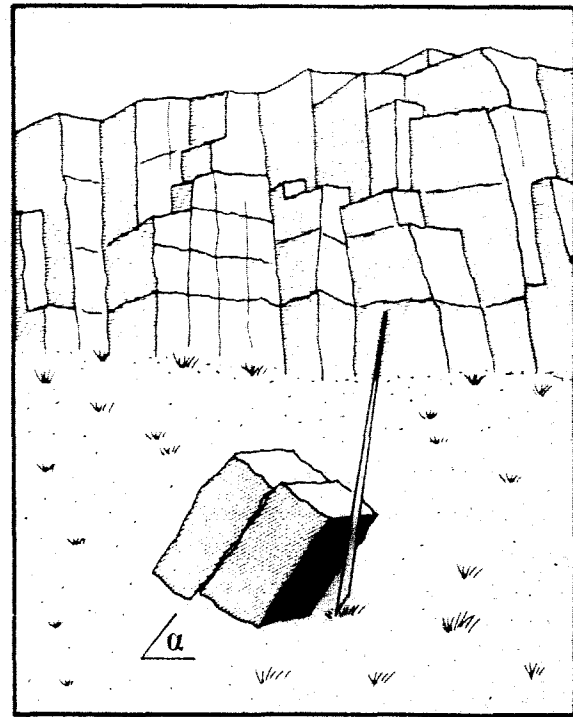
TILT TEST

Fig. 29. A simple method for obtaining a scale-free value of JRC when the natural rock blocks are not too large or difficult to extract.

angle (ϕ_r). The value of JCS can be predicted from Schmidt hammer tests [26], but an allowance should be made for a scale effect.

Barton & Choubey [12] have proposed a tentative range of scale reduction factors of 2.5, 5 and 10, the maximum suggested for cases of porous weathered rock types and the minimum for dense, hard rocks. The Schmidt hammer results can also be used to predict the value of ϕ_r from

$$\phi_r = (\phi_b - 20°) + 20\,(r/R) \tag{4}$$

where

r = rebound no. of the weathered joint wall (saturated)

R = rebound no. of dry unweathered surfaces of the rock

The basic friction angle (ϕ_b) applies to dry unweathered flat surfaces and can be measured by tilt testing of rough-sawn blocks; or by tilting sets of three drill-core sticks of the rock in question with the core pieces held to form a 'triangle' with the upper core sliding along its line contacts with the lower two (Stimpson, B. Personal communication, 1979).

In the case of a pull test (which may be preferable for joints of high JRC) the top block is pulled parallel to the horizontal or inclined joint plane (Fig. 30). The external pulling force (T_2) can be applied via a grouted bolt and hook and care should be taken to apply the necessary force close to the joint plane to avoid moments. Joint-block preparation will probably require line-drilling to remove the stabilizing effect of interlock-
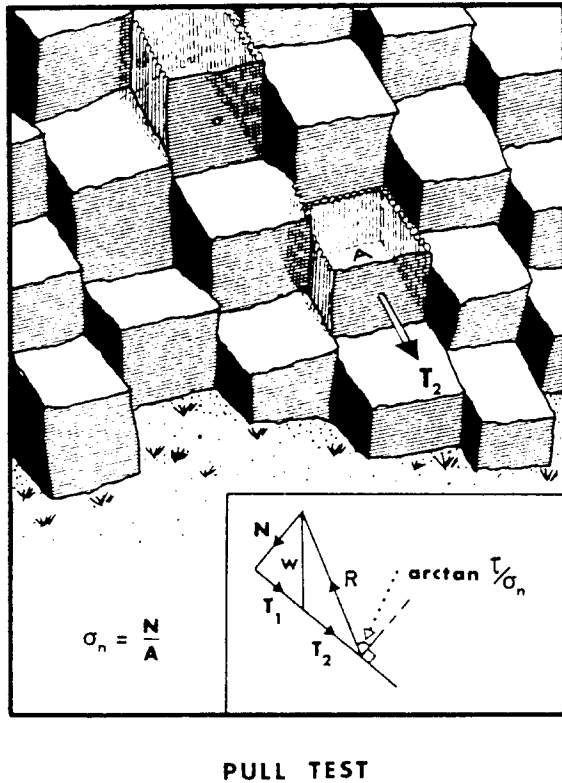
PULL TEST

Fig. 30. Another simple method for obtaining a scale-free value of JRC when the natural rock blocks are large and/or too rough for tilt testing.

ing asperities from the surrounding blocks. The relevant value of JRC can be obtained from:

$$JRC = \frac{\tan^{-1}\left(\dfrac{T_1 + T_2}{N}\right) - \phi_r}{\log_{10}\left(\dfrac{JCS \times A}{N}\right)} \qquad (5)$$

where

T_1 = tangential component of the self-weight of the overlying block (for inclined joint planes)

T_2 = external pulling force (or pushing force if applied via a flat jack inserted between the line-drilled walls of two adjacent blocks = 'push' test)

N = normal component of block weight (W)

A = joint area

Equation (2) can then be used to predict the complete peak shear strength envelope over the desired level of normal stress.

It is important to note that in estimating JRC from equations (3) or (5) the input values for JCS and ϕ_r need not be very accurate. Since the ratio of JCS/σ_n would probably be in the range of 1000–100,000 in most conceivable cases, the error in the estimate of ϕ_r would be reduced by a factor of 3–5. Also, the error in estimating the full-scale value of JCS would be relatively small due to the logarithmic formulation. In each case, equations (3) or (5) ensure an automatic compensation for overestimates or underestimates of ϕ_r and/or JCS by producing underestimated or overestimated values for JRC, since the three components combined (JRC, JCS, ϕ_r) have to constitute the measured strength. The errors in the values of peak arctan $(\tau/\sigma_n)^2$ predicted at the required engineering levels of normal stress (σ_n) would be relatively small (e.g. [12]).

Correction of JRC values measured on laboratory samples

It may not always be possible to conduct large-scale (natural block size) tilt, push or pull tests. A method is needed to extrapolate laboratory JRC values to longer
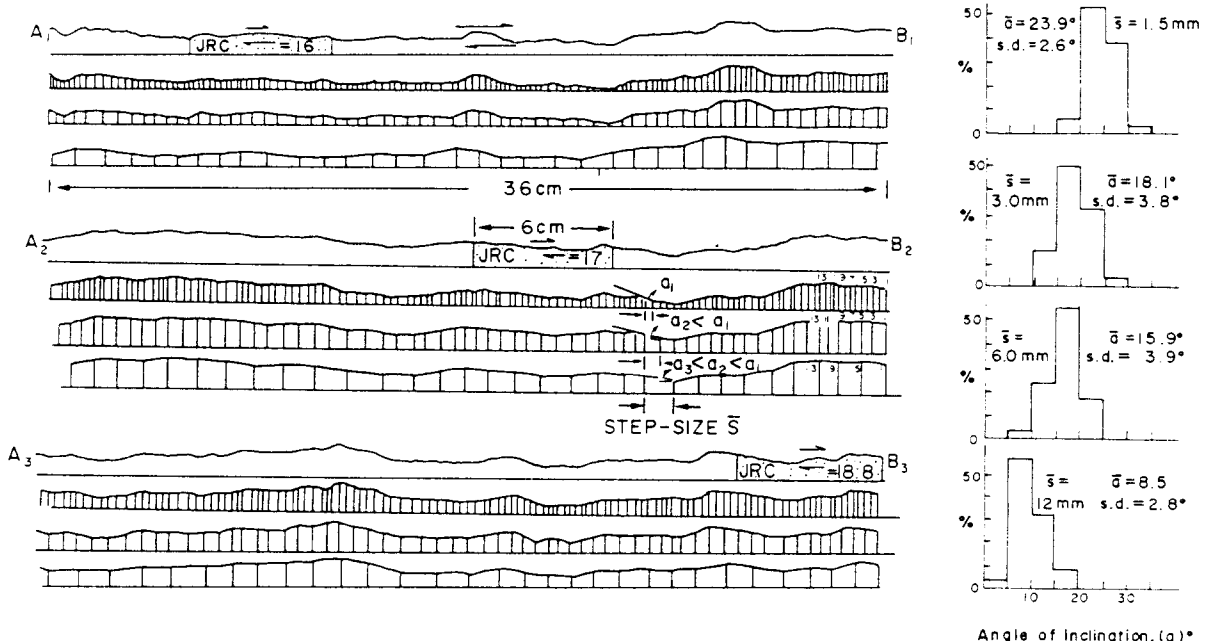

Fig. 31. Example from model No. 1, showing the variations in the asperity inclination angle ($\bar{a}$) with step size ($\bar{s}$). A step size of about 2% of the joint length corresponds to the critical asperities controlling JRC and peak shear strength.

profiles measured in the field to supplement the experimental trends shown in Fig. 22.

Rengers [21] and Barton [20] analysed joint roughness by dividing surface roughness profiles into different stepsizes, thereby sampling asperities of different steepness and base length. Larger step-sizes linearize the small steep asperities, thereby sampling only the longer and more gently inclined asperities.

Analyses of the present joint replicas at different scale (i.e. 6 cm and 36 cm lengths) indicates that the mean inclination angles $(\bar{a}°)$ of asperities sampled with step-sizes approximately 2% of the length of each specimen gives the following simple relation:

$$JRC_{36}/JRC_6 = \bar{a}_{36}^2/\bar{a}_6^2 \qquad (6)$$

In the example shown in Fig. 31, the 1.5 mm step-size on the 6 cm profiles gives $\bar{a}_6 = 23.9°$, while the measured value of JRC_6 is 17.7. The 9.0 mm (6 × 1.5) step-sizes on the 36 cm specimen gives $\bar{a} = 15.9°$, and therefore the value of JRC_{36} predicted from equation 6 is 17.7 (23.9/15.9) = 11.8. The measured value of JRC_{36} is 12.0. Similar good agreement is found for a large range of joint types.

In practice the following form of equation (6) is recommended for obtaining a more or less scale free value of JRC based on a 2% step-size.

$$JRC_{natural\ block}/JRC_{laboratory} = \bar{a}_{natural\ block}°/\bar{a}_{laboratry}°$$

The value of JRC_{lab} can readily be obtained from small scale tilt tests.

CONCLUSIONS

(1) The peak shear strength (τ_p) of rock joints is a strongly scale-dependent property. Its inverse relationship with joint length is non-linear and tends to become asymptotic.

(2) Increasing scale alters the shearing characteristics significantly. The peak shear displacement (d_{hp}) increases, behaviour changes from 'brittle' to 'plastic' and smaller displacement is required to reach the ultimate strength (τ_{ult}). For practical purposes d_{hp} can be taken as approximately equal to 1% of the joint length for a large range of block sizes and types of roughness.

3. Both the geometrical and strength characteristics of surface roughness are potential sources of scale effect. The small and steep asperities regulate the peak shearing path of short joints, whereas larger but flatter features become effective for correspondingly larger joints. Present indications are that the average base length of critical asperities is about 4% of the joint length. The involvement of different asperity sizes causes development of more gently inclined and larger individual contact areas at the instant of peak strength as the scale increases. As a result, both the joint roughness coefficient (JRC) and joint compression strength (JCS) reduce significantly with increasing joint length. By implication the variables—peak dilation $(d_n°)$, asperity failure component $(S_A°)$ and of course the peak friction angle (arctan τ_p/σ_n)—are all scale dependent.

(4) The magnitude of these effects depends on the type of roughness. Maximum scale effects are associated with rough undulating joints, and minimum with almost smooth and planar types.

(5) Differences may exist between the behaviour of individually sheared joints and the collective performance of the large number of blocks in a multi-jointed mass. Despite equal joint roughness the shear strength of a densely jointed mass (small block size) may be higher than that of a wider jointed mass (large block size). This scale effect is related to the changing mass stiffness as the block size increases or decreases. Small blocks have greater capacity to rotate slightly and maintain contact with small-scale features of roughness, hence their higher shear strength.

(6) There are reasons to suggest that the naturally occurring block-size as defined by the spacing of cross-joints may constitute a potential scale effect size limit, and therefore also the most relevant joint length to test or analyse. Tilt or pull tests on singly jointed blocks of length equal to the mean joint spacing are two inexpensive methods of deriving almost scale-free estimates of JRC. If these large scale index tests are not technically feasible, the JRC values measured in the laboratory can be corrected by conducting simple roughness analyses.

REFERENCES

1. Schneider H. J. The laboratory direct shear test—an analysis and geotechnical evaluation. *Bull. int. Ass. Engng Geol.* **18**, 121–126 (1978).
2. Deere D. U., Hendron A. J., Patton F. D. & Cording E. J. Design of surface and near-surface construction in rock. *Proc. 8th Symp. Rock Mechanics on Failure and Breakage of Rock.* Minnesota. (Edited by C. Fairhurst) Chap. 11, pp. 237–302 (1967).
3. Salas J. A. J. Mechanical resistances. *Proc. Int. Symp. on Rock Mechanics.* Madrid. Theme 2, pp. 115–130 (1968).
4. Jaeger J. C. Friction of rocks and the stability of rock slopes. *Géotechnique* **21**, 97–134 (1971).
5. Wareham B. F. & Sherwood D. E. The relevance of size of sample and type of test in determining shear properties for use in stability analysis. *Proc. 3rd Congr. Int. Soc. for Rock Mechanics.* Denver, CO. Vol. IIA, pp. 316–321 (1974).
6. Londe P. The role of rock mechanics in the reconnaisance of rock foundations. *Q. Jl Engng Geol.* **6**, 57–74 (1973).
7. Infanti N. & Kanji M. A. *In-situ* shear strength, normal and shear stiffness determinations at Agua Vermelha Project. *Proc. 3rd Int. Congr. of Int. Ass. of Engineering Geology.* Madrid. Session 2, Vol. 2, pp. 175–183 (1978).
8. Krsmanovic D. & Popovic M. Large-scale field tests of the shear strength of limestone. *Proc. 1st Congr. Int. Soc. for Rock Mechanics.* Lisbon. Vol. 1, pp. 773–779 (1966).
9. Pratt H. R., Black A. D. & Brace W. F. Friction and deformation of jointed Quartz Diorite. *Proc. 3rd Congr. Int. Soc. for Rock Mechanics.* Denver, CO. Vol IIA, pp. 306–310 (1974).
10. Locher H. G. & Rieder U. G. Shear tests on layered Jurassic Limestone. *Proc. 2nd Congr. Int. Soc. for Rock Mechanics.* Belgrade. Vol. 2, Paper 3–1 (1970).
11. Brown E. T., Richards L. R. & Barr M. V. Shear strength characteristics of the Delabole slates. *Proc. Conf. on Rock Engineering.* Newcastle. pp. 33–51 (1977).
12. Barton N. & Choubey V. The shear strength of rock joints in theory and practice. *Rock Mech.* **10**, 1–54 (1977).
13. Barton N. The shear strength of rock and rock joints. *Int. J. Rock Mech. Min. Sci. & Geomech. Abstr.* **13**, 255–279 (1976).
14. Bandis S. Experimental studies of scale effects on shear strength, and deformation of rock joints. Ph.D. Thesis, The University of Leeds, Department of Earth Sciences (1980).

15. Obert L. & Duval W. I. *Rock Mechanics and the Design of Structures in Rock*. Wiley, New York (1967).
16. Deere D. U. Geological considerations. *Rock Mechanics in Engineering Practice*. Chap. 1, 1–20 (1974).
17. Barton N. Review of a new shear strength criterion for rock joints. *Engng Geol.* 7, 287–332 (1973).
18. Mogilevskaya S. E. Morphology of joint surfaces in rock and its importance for engineering geological examination of dam foundations. *Proc. 2nd Congr. Int. Ass. of Engineering Geology*. Sao Paolo, Brazil. Theme VI, pp. 17.1–17.8 (1974).
19. Patton F. D. Multiple modes of shear failure in rock and related materials. Ph.D. Thesis. University of Illinois, p. 282 (1966).
20. Barton N. A relationship between joint roughness and joint shear strength. *Proc. Int. Symp. on Rock Mechanics*, Nancy. Paper 1–8 (1971).
21. Rengers N. Influence of surface roughness on the friction properties of rock planes. *Proc. 2nd Int. Soc. for Rock Mechanics*. Belgrade. Vol. 1, Paper 1–31 (1970).
22. Lama R. D. & Gonano L. P. Size-effect considerations in the assessment of mechanical properties of rock masses. *Proc. 2nd Symp. on Rock Mechanics*. Dhanbad (1976).
23. Broch E. & Franklin J. A. The point-load strength test. *Int. J. Rock Mech. Min. Sci.* 9, 669–697 (1972).
24. Einstein H. H., Baecher G. B. & Hirschfeld R. C. The effect of size on strength of a brittle rock. *Proc. 2nd Congr. Int. Soc. for Rock Mechanics*. Belgrade. Paper 3–17 (1970).
25. Barton N. R. A model study of rock joint deformation. *Int. J. Rock Mech. Min. Sci.* 9, 579–602 (1972).
26. International Society for Rock Mechanics. Commission on Standardization of Laboratory and Field Tests. Suggested methods for determining hardness and abrasiveness of rocks. *Int. J. Rock Mech. Min. Sci. Geomech. Abstr.* 15, 89–99 (1978).